

Other Materials Data

İstemihan Gökdağ and Erdem Acar*

Application of a modular topology optimization framework to an aerospace bracket design

<https://doi.org/10.1515/mt-2021-2148>

Abstract: In aerospace industry, optimizing designs has become inevitable in terms of weight and performance requirements. Topology optimization is the most suitable optimization type for use in the conceptual design phase. Even though academic topology optimization algorithms have a modular structure (open to development), they are often useable for a regular design domain. Alternatively, commercial topology optimization software products, on the other hand, are very useful in terms of their solution speed, accuracy, and ability to handle complex or irregular design domains. However, the user is restricted with the optimization algorithms available in the software, and these software do not usually have a modular structure. In this study, a modular topology optimization framework that combines useful features of the academic codes (e.g., modularity) and the commercial software tools (e.g., capability of easily handling complex design domains) is developed. The developed framework is tested on two popular academic topology optimization problems, followed by aerospace bracket design problem. It is observed that the proposed framework usually provides lower objective function values and converges to the optimum result in fewer iterations than the Altair Optistruct topology optimization software.

Keywords: aerospace bracket design; irregular design domain; modular framework; structural optimization; topology optimization.

1 Introduction

Size, shape and topology optimization methods deal with the structural design process in different ways [1]. In a standard size optimization problem, the optimum thickness of a plate or the optimum cross-sectional area of truss elements can be found [2]. For instance, Aslan and Yıldız [3] used size optimization techniques to obtain optimum dimensions of an automobile suspension arm. In shape optimization problems, the geometric variables of the determined design elements are seen as the elements that determine the optimum design [4]. In a recent study, Yıldız et al. [5] performed optimum shape design of automobile suspension components using butterfly optimization algorithm. Topology optimization, on the other hand, is used to determine the number of holes specified in the design space, their location, shape and their connection with the design space [6]. Since topology optimization finds the optimum material distribution that minimizes an objective function value in the design space, it is considered as a prerequisite for size and shape optimization.

Topology optimization has experienced an explosive growth since its introduction in the seminal paper by Bendsoe and Kikuchi [7]. Topology optimization approaches can be categorized into density based methods [6, 8], level-set based methods [9, 10], topological derivatives based methods [11–13], phase field approaches [14, 15], and evolutionary approaches [16–18]. A comprehensive review of topology optimization approaches can be found in Sigmund and Maute [19]. Also, the reader is referred to Zhu et al. [20] for a recent review of research on the integration of topology optimization and additive manufacturing.

Topology optimization methods has also shown an extensive range of applications in engineering over the last years, and the recent applications include the following studies. Yıldız [21] performed optimal structural design of vehicle components using topology optimization. Cavazzuti et al. [22] used topology optimization methods to achieve high performance automotive chassis design. Dede et al. [23] performed topology optimization,

*Corresponding author: Erdem Acar, Mechanical Engineering, TOBB University of Economics and Technology, Sogutozu Cad. No:43, Cankaya, Ankara, Ankara, 06560, Turkey, E-mail: erdem.acar@gmail.com. <https://orcid.org/0000-0002-3661-5563>

İstemihan Gökdağ, TOBB University of Economics and Technology, Ankara, Ankara, 06120, Turkey; and Turkish Aerospace Industries Inc., Additive Manufacturing Division, Ankara, 06980, Turkey

additive layer manufacturing, and experimental testing of an air-cooled heat sink. Dilgen et al. [24] presented a fast and viable approach for taking into account turbulence in topology optimization of complex fluid flow systems. Cheng et al. [25] performed topology optimization of functionally graded lattice structures for the design of additive manufactured components with stress constraints. Yıldız et al. [26] used topography and topology optimization techniques to obtain lightweight design of diesel engine components. Kollman et al. [27] developed a deep learning model for topology optimization of 2D metamaterials.

Topology optimization algorithms are often tested on numerical examples with a regular design domain, i.e., shape of the design domain is simple. For instance, top99 code [28] and TOP3D code [29], both developed in MATLAB, are widely used in the literature for academic application problems, have very high success in terms of solution speed and final topology. These codes have a modular structure such that they are open to development. That is, one can easily tailor these codes for his/her problem of interest. However, these codes can only solve problems in a simple design domain (e.g., rectangular prism for a 3-D design space). Irregular design space problems can be handled by inserting some non-designable hole areas and applying length scale control. However, the complex shape of the irregular design domain might conflict with the length scale requirement, leading to convergence issues. Even though this problem could be solved by employing a dynamic length scale control, this control strategy might not be easily implemented to every topology optimization algorithm.

Commercial topology optimization software products have their own finite element (FE) analysis modules. ANSYS, Genesis, Msc.Nastran and OptiStruct are widely known examples of these software tools. These software products are very useful in terms of their solution speed, accuracy, and ability to handle complex or irregular design domains. Even though these software are user friendly and easy to use, the user is restricted with the optimization algorithms available in the software, and they do not have a modular structure that is open to development.

The objective of this paper is to develop a modular topology optimization framework that combine useful features of the academic codes (e.g., modularity) and the commercial software tools (e.g., capability of easily handling complex design domains). The remainder of the paper is structured as follows: Basic formulation of a topology optimization problem is presented in the next section. Modular topology optimization framework developed in this study is explained in Section 3. The results

of the application of the proposed modular topology optimization framework on two popular academic test problems and an industrial application problem (aviation bracket design problem) is presented in Section 4.

2 Basic topology optimization formulation

The basic formulation of a topology optimization problem can be defined as follows [6]:

$$\begin{aligned} & \text{Minimize } f(\boldsymbol{\rho}) \\ & \text{Subject to } \int_{\Omega} \rho \, dv \leq \bar{V} \\ & \boldsymbol{\rho} = \mathbf{0} \text{ or } \mathbf{1}, \forall v \in \Omega \end{aligned} \quad (1)$$

with $\boldsymbol{\rho}$: Design variable vector that consists of the artificial density value of each element.

The function $f(\boldsymbol{\rho})$ in Equation (1) is the objective function, and often compliance is used as the objective function in many structural optimization studies. The main constraint function in Equation (1) is the volume constraint that states that the design volume should not exceed a pre-specified value \bar{V} . The other constraint function in Equation (1) states that the density variable $\rho(v)$ can take either the value 0 (void) or 1 (solid material) at any design domain Ω .

In the density-based approach, the most frequently used approach in the literature, the problem is defined by using artificial density values to find the optimum material distribution. The most common density-based methods are the homogenization method [7, 8, 30, 31] and the SIMP method [32, 33]. In density-based approaches, the design is expressed in two or more phases, one of which is the void phase. In the discretized design space, the mechanical properties of the material are calculated using a power law that interpolates between solid and space [34]. This power law is defined as the Solid Isotropic Material with Penalization (SIMP) method in the literature. The modulus of elastic of each element is calculated by Equation (2) specified in the standard SIMP method as follows [6]:

$$\mathbf{E}_i = \mathbf{E}(\boldsymbol{\rho}_i) = \boldsymbol{\rho}_i^p \mathbf{E} \quad (2)$$

with $\boldsymbol{\rho}_i$: Artificial density value of each element, \mathbf{E} : Elastic modulus of the solid material and p : Penalty factor.

In this study, the penalty factor is chosen as $p = 3$ following Bendsoe and Sigmund [6]. In a finite element split design, filters need to be added to the problem in order to define the relationship of elements with neighboring elements and to eliminate checkerboard effects [35]. In addition, a modified SIMP method was created by adding an element with a low elastic modulus to the equation to

avoid the singularity problem during the FE analysis. The modified SIMP method offers many advantages for adding filters and the formulation in Equation (3) is used [36].

$$\mathbf{E}_i = \mathbf{E}(\rho_i) = \rho_i^p (\mathbf{E}_0 - \mathbf{E}_{\min}) + \mathbf{E}_{\min} \quad (3)$$

with \mathbf{E}_0 : Elastic modulus of the solid material and \mathbf{E}_{\min} : Elastic modulus of the void material (non-zero in order to avoid singularity).

Nonlinear programming problems with minimum flexibility objective function, used quite frequently in topology optimization, can be solved by sequential convex approaches such as sequential quadratic programming [37] and method of moving asymptotes, MMA [38]. The Optimality Criteria method, a historically older method, is still one of the most used methods due to its numerical simplicity and efficiency [39].

As noted earlier, even though academic codes have very high success in terms of solution speed and final topology, and have a modular structure such that they are open to development, they can usually solve problems in a simple design domain. Their use in irregular design space problems is not straightforward. On the other hand, commercial topology optimization software products can easily handle complex or irregular design space problems, but they do not have a modular structure. In this study, a modular topology optimization framework that combine useful features of the academic codes (e.g., modularity) and the commercial software tools (e.g., capability of easily handling complex design domains) is developed. The details of the developed modular topology optimization framework are presented in the next section.

3 Proposed modular topology optimization framework

Topology optimization problems can be formulated in different ways according to the objective and constraint functions. In this study, the minimum compliance problem is used to find the optimum design topology. The objective is to generate the minimum strain energy in the constrained volume of the design under the applied forces. The minimum compliance problem can be formulated as [28]:

$$\begin{aligned} & \text{Minimize } \mathbf{C}(\boldsymbol{\rho}) = \mathbf{u}^T \mathbf{K}(\boldsymbol{\rho}) \mathbf{u} \\ & \text{Subject to } \mathbf{K}(\boldsymbol{\rho}) \mathbf{u} = \mathbf{f} \\ & \sum_{i=1}^N \rho_i v_i - \bar{V} \leq 0 \\ & 0 \leq \rho_{\min} \leq \rho_i \leq 1, \quad i = 1, \dots, N \end{aligned} \quad (4)$$

with $\boldsymbol{\rho}$: Artificial density vector containing all the design variables, \mathbf{C} : Compliance matrix of the structure, \mathbf{K} : Global

stiffness matrix, \mathbf{u} : Displacement vector, \mathbf{f} : External force vector, ρ_i and v_i : Artificial density and the volume of the finite element, respectively, N : Total number of elements, \bar{V} : Constrained volume of the design space and ρ_{\min} : Number close to zero to avoid the singularity problem.

The modulus of elasticity of each element is calculated by Equation (3).

Since the formulated topology optimization problem is often solved by a gradient-based optimization method, derivatives of the elasticity matrix according to $C(\boldsymbol{\rho})$ design variables are needed. Derivatives are calculated with the adjoint variable method as stated in Equations (5) and (6):

$$\frac{\partial \mathbf{C}(\boldsymbol{\rho})}{\partial \rho_i} = -\mathbf{u}^T \frac{\partial \mathbf{K}(\boldsymbol{\rho})}{\partial \rho_i} \mathbf{u} \quad (5)$$

$$\begin{aligned} \frac{\partial \mathbf{K}(\boldsymbol{\rho})}{\partial \rho_i} &= \frac{\partial}{\partial \rho_i} \sum_{i=1}^N [\mathbf{E}_{\min} + \rho_i^p (\mathbf{E}_0 - \mathbf{E}_{\min})] \mathbf{K}_i^0 \\ &= p \rho_i^{p-1} (\mathbf{E}_0 - \mathbf{E}_{\min}) \mathbf{K}_i^0 \end{aligned} \quad (6)$$

with \mathbf{K}_i^0 : Global stiffness matrix.

If this matrix is substituted into Equation (6), then Equation (7) that reduce it from the global level to the element level can be obtained as follows:

$$\frac{\partial \mathbf{C}(\boldsymbol{\rho})}{\partial \rho_i} = -p [\rho_i^{p-1} (\mathbf{E}_0 - \mathbf{E}_{\min})] \mathbf{u}_i^T \mathbf{K}_i \mathbf{u}_i \quad (7)$$

with \mathbf{u}_i : Displacement at the nodes of a finite element and \mathbf{K}_i : Local stiffness matrix of that element.

Numerical difficulties such as mesh-dependency, checkerboard pattern and local minimum are encountered in the topology optimization method [6]. Density filter method, which is a widely used type of editing techniques, is used to reduce numerical difficulties. In this study, the density filter function [40] stated in Equation (8) is used:

$$\tilde{x}_i = \frac{\sum_{j \in N_i} \mathbf{H}_{ij} v_j x_j}{\sum_{j \in N_i} \mathbf{H}_{ij} v_j} \quad (8)$$

with N_i : Neighborhood term of the finite element x_i with volume v_i .

When calculating the neighborhood term, firstly, the distance between the center of each finite element and the centers of all other finite elements is calculated. Then, the distance function, \mathbf{H}_{ij} , between a given filter size, \mathbf{R} , and neighboring elements, which acts as a weighting factor, is calculated using Equation (9) following Liu and Tovar [29].

$$\mathbf{H}_{ij} = \mathbf{R} - \text{dist}(\mathbf{i}, \mathbf{j}) \quad (9)$$

with \mathbf{R} : Neighborhood size or filter size, and the function $\text{dist}(\mathbf{i}, \mathbf{j})$: Distance between the centers of the finite element \mathbf{i} , and the finite element \mathbf{j} .

When defining the neighborhood term, the cases where the distance between the centers of the finite elements is less than the specified filter size [29] are examined and expressed as in Equation (10):

$$N_i = \{j : \text{dist}(\mathbf{i}, \mathbf{j}) \leq R\} \quad (10)$$

One of the difficulties of topology optimization is to integrate the problem with many design variables, and medium-sized constraint functions into mathematical programming [6]. The MMA algorithm [38], which gives very good results in a short time for large-scale topology optimization problems, is used in this study. The flowchart of the topology optimization framework developed in this study (named as IGEA method, reflecting the initials of the authors) is given in Figure 1.

The detailed explanations of the steps in the flowchart, which is fully automated using MATLAB software, are as follows:

- (1) The design variables determined by the user in the first iteration are updated by the optimization algorithm at each iteration.
- (2) Since the densities of all finite elements are the design variables of the optimization problem, the elasticity modulus specific to each element is calculated from Equation (3), used in the modified SIMP method, and assigned to the relevant element using the material property card.
- (3) The elasticity modulus values, the input of the material cards, are entered into the input file of an FE preprocessor. In this study, we use Hypermesh software as the FE processor, but any FE preprocessor can be used within this modular framework. The created input file is loaded into the Hypermesh software automatically, and then FE analysis is performed. In this study, we use HyperWorks Optistruct solver as the FE solver, but any FE solver can be used within this modular framework. After all processes are completed, the program is closed.
- (4) The objective function specified globally in Equation (2) can be expressed by Equation (11) at the element level. Notice that the compliance is the sum of the strain energy of each finite element.

$$C(\boldsymbol{\rho}) = \mathbf{u}^T \mathbf{K}(\boldsymbol{\rho}) \mathbf{u} = \sum_{i=1}^N \mathbf{u}_i^T \mathbf{K}_i \mathbf{u}_i \quad (11)$$

- (5) The volume constraint function is calculated from Equation (12) at each iteration, and it is ensured that the constraint is violated.

$$\sum_{i=1}^N \boldsymbol{\rho}_i \mathbf{v}_i - \bar{V} \leq 0 \quad (12)$$

- (6) Since the MMA optimization algorithm is a gradient-based algorithm, the derivatives of the objective function must be calculated according to the design variables. These derivatives are calculated using Equation (13). Derivatives calculated with the density filter used in order to reduce the numerical difficulties specified in Equation (8) are filtered and input into the optimization.

$$\frac{\partial C(\boldsymbol{\rho})}{\partial \boldsymbol{\rho}_i} = -\mathbf{p} [\boldsymbol{\rho}_i^{p-1} (\mathbf{E}_0 - \mathbf{E}_{\min})] \mathbf{u}_i^T \mathbf{K}_i \mathbf{u}_i \quad (13)$$

- (7) The objective and constraint functions as well as their derivatives with respect to the filtered design variables are fed into the optimizer, and values of the design variables for the next iteration are computed (i.e., design variables are updated). The updated design variables are filtered using the density filter before starting the new iteration, and steps in the flowchart are followed until convergence is achieved.

4 Results

The accuracy and efficiency of the IGEA method is first tested on two frequently used academic problems in the literature: the fixed beam problem, and the Messerschmitt–Bolkow–Blohm (MBB) beam problem. Then, the IGEA method is applied to an industrial application problem: aviation bracket design. All these problems are solved using both the IGEA method and the Altair Optistruct topology optimization software (Version 2017.2), and the results are compared. In Optistruct, the following settings are used for all problems: dual algorithm based on separable

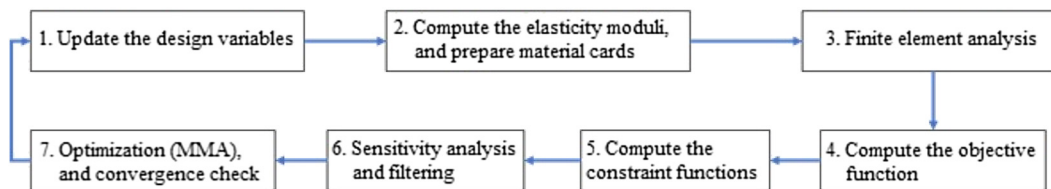


Figure 1: Flowchart of the modular IGEA topology optimization framework.

convex approximation is used as optimization method, convergence check is included in optimization setup using the control card of relative convergence criterion, and the value of ρ_{\min} is adjusted using minimum material density parameter. The same convergence check for compliance is used for both IGEA and Optistruct, and this value is varied for different problems. Similarly, minimum element density is taken as $\rho_{\min} = 0.01$ in both IGEA and Optistruct solutions.

4.1 The fixed beam problem

The fixed beam problem is indicated in Figure 2. The beam is fully fixed at the right end, and loaded at the other end with a constant distributed (along the z -axis) load of 5000 N. The beam is divided into 600 finite elements in total by using 30, 10 and 2 elements in the x , y and z axis, respectively. The parameter in volume constraint is taken as $\bar{V} = 0.7$. That is, the ratio of the final volume to the initial volume should be 0.7 (i.e., the optimum design should be at least 30% lighter than the initial design). The beam is optimized for minimum compliance.

In IGEA method, the values of the artificial densities (i.e., design variables) of all elements is taken as 0.7 (the volume ratio) in the first iteration of MMA algorithm. The optimization process is continued until the relative change of the objective function between the two consecutive iterations is less than 10^{-6} . In Optistruct, the default optimization settings are used.

Figure 3 shows the variation of the objective function (compliance) with respect to iterations for the fixed beam problem, solved by using both IGEA and Optistruct. It is seen that IGEA yields a smaller compliance value than Optistruct. It is also seen that IGEA is converged in 31 iterations, whereas Optistruct is converged in 202 iterations.

The optimum topologies obtained by using IGEA and Optistruct are shown in Figure 4. Note that the raw results (i.e., topologies corresponding to the values of design variables in the last iteration) are used in comparison, because post-processor of Optistruct uses an extra filter when visualizing the final topology. Figure 4 shows that the optimum topologies obtained using IGEA and Optistruct are similar to each other in general terms. However, as noted earlier, IGEA yields smaller compliance values than Optistruct.

4.2 The MBB beam problem

The initial design, loading and boundary conditions for the MBB beam problem are shown in Figure 5. The beam is simply supported at both ends, and a constant distributed (along z -axis) load of 1 N is applied to the beam in the middle. The beam is divided into 600 finite elements in total by using 30, 10 and 2 elements in the x , y and z axes, respectively. As in Problem #1, the parameter in volume constraint is taken as $\bar{V} = 0.7$. The beam is optimized for minimum compliance.

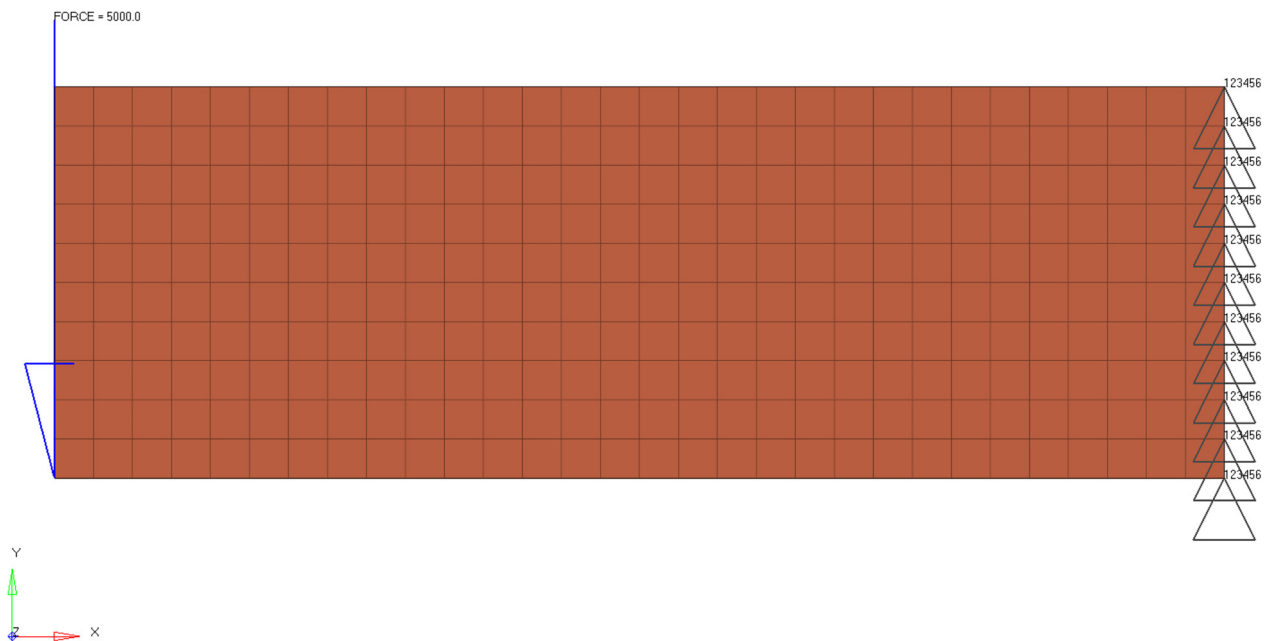


Figure 2: Initial design, loading and boundary conditions for the fixed beam problem.

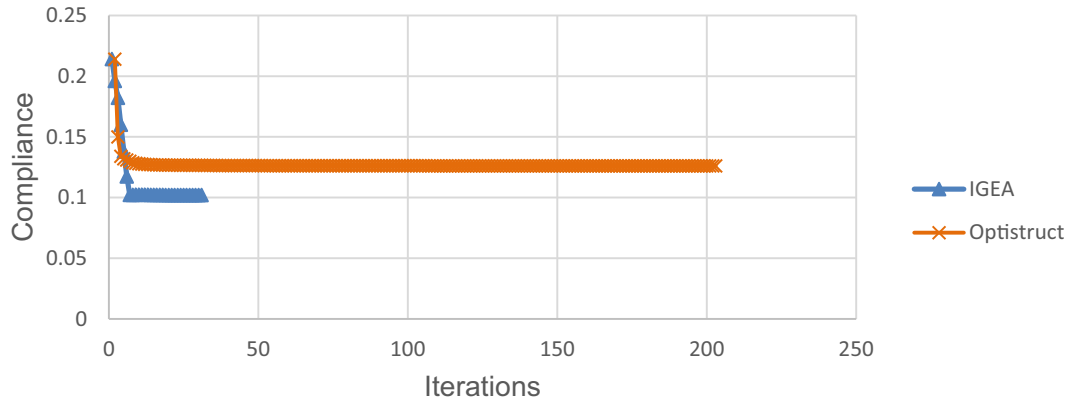


Figure 3: Variation of the objective function (compliance) with respect to iterations for the fixed beam problem.

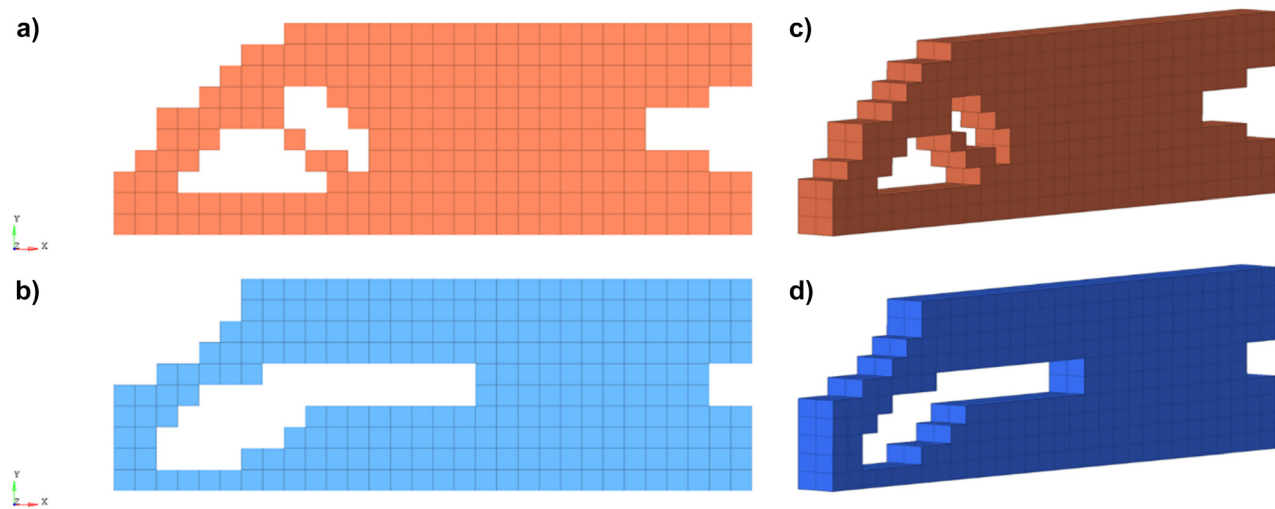


Figure 4: Fixed beam, a) front view of the optimum topology obtained with Optistruct, b) front view of the optimum topology obtained with IGEA, c) Isometric view of the optimum topology obtained with Optistruct, d) Isometric view of the optimum topology obtained with IGEA.

The variation of the objective function with respect to the iterations is given in Figure 6. It is found that the optimum compliance obtained with IGEA is 0.86 times smaller than that of the Optistruct. It is also found that IGEA converges to the optimum result in six iterations, while the Optistruct converges in nine iterations.

Figure 7 shows that the optimum topologies obtained using IGEA and Optistruct are similar in outline, whereas the IGEA optimum has a hole in the middle. However, when the result of the Optistruct software is examined in detail, when the front row of elements is masked in the z -axis with 10 elements, the optimum design attained by Optistruct has also a gap in the middle, as shown in Figure 8.

4.3 Aviation bracket design

Finally, topology optimization of an aviation bracket is studied as an application problem. This bracket is aimed to be used in aerospace products (not explicitly stated due to confidentiality) produced by Turkish Aerospace Industries. The design volume is given as 0.2, 0.1 and 0.03 m in the x , y and z axes, respectively. A constant distributed load of 100 N is applied to the hole (shown in Figure 9) along x and y axes, and fixed support conditions are applied at the left end as shown in Figure 9.

The bracket is to be manufactured through additive manufacturing. The material of the bracket is 30 μm AlSi10Mg powder provided by SLM Solutions [41], which

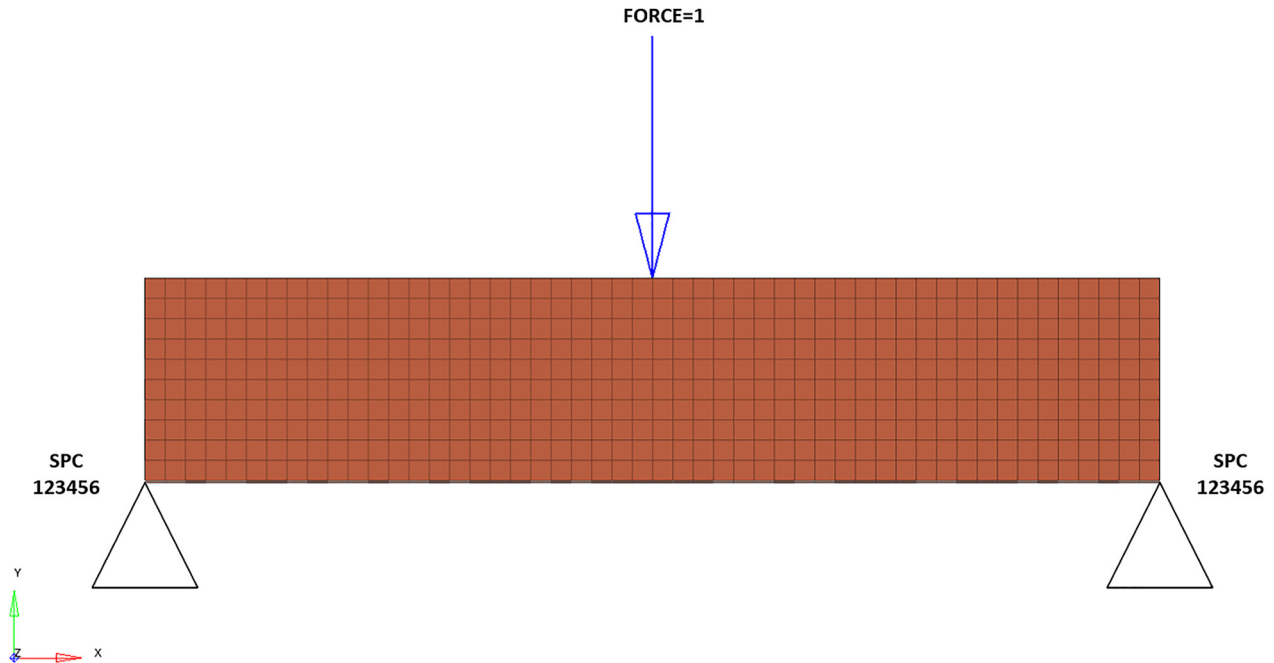


Figure 5: Initial design, loading and boundary conditions for the MBB beam problem.

has properties close to aluminum material suitable for aviation quality, and its mechanical properties are presented in Table 1. Samples are produced by using three different manufacturing angles: 0° (horizontal), 45° , and 90° (vertical), and tensile tests are performed to obtain the modulus of elasticity and the yield stress according to DIN EN ISO 6892-1 using Zwick 1484 testing machine [41]. It is found that the lowest mechanical properties are attained when the manufacturing angle is 90° . Therefore, these mechanical property values are used in design of this part, to be conservative.

The aviation bracket is modeled with a total of 58,224 finite elements, and the optimization problem specified in

Equation (4) is solved using both IGEA and Optistruct. The compliance (strain energy sum of all elements) is used as the objective function, the force equation from Hooke's law is used, \bar{V} is taken as 0.7. The optimization iterations are continued until the relative change of the objective functions between the two consecutive iterations is less than 10^{-3} .

The variation of the objective function with respect to the iterations is given in Figure 10. It is found that the optimum compliance value obtained using IGEA is 0.87 times smaller than that of the Optistruct. It is also observed that IGEA converges to the optimum result in six iterations, whereas Optistruct converges in 15 iterations.

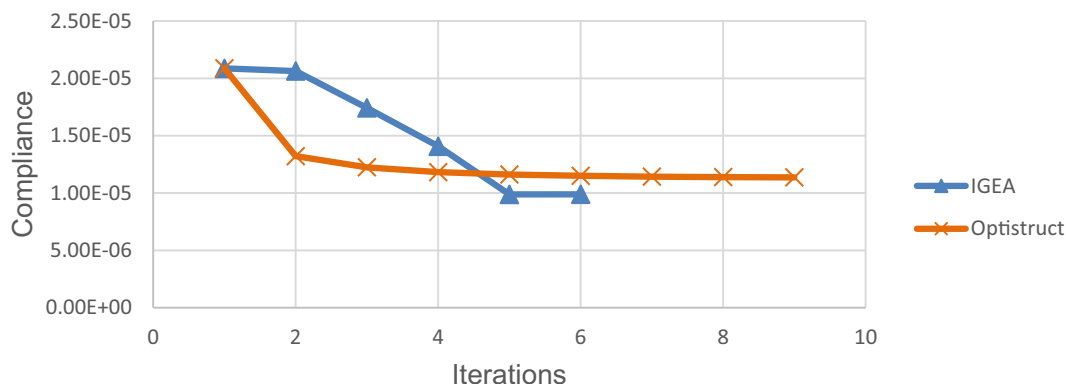


Figure 6: Variation of the objective function (compliance) with respect to iterations for the MBB beam problem.

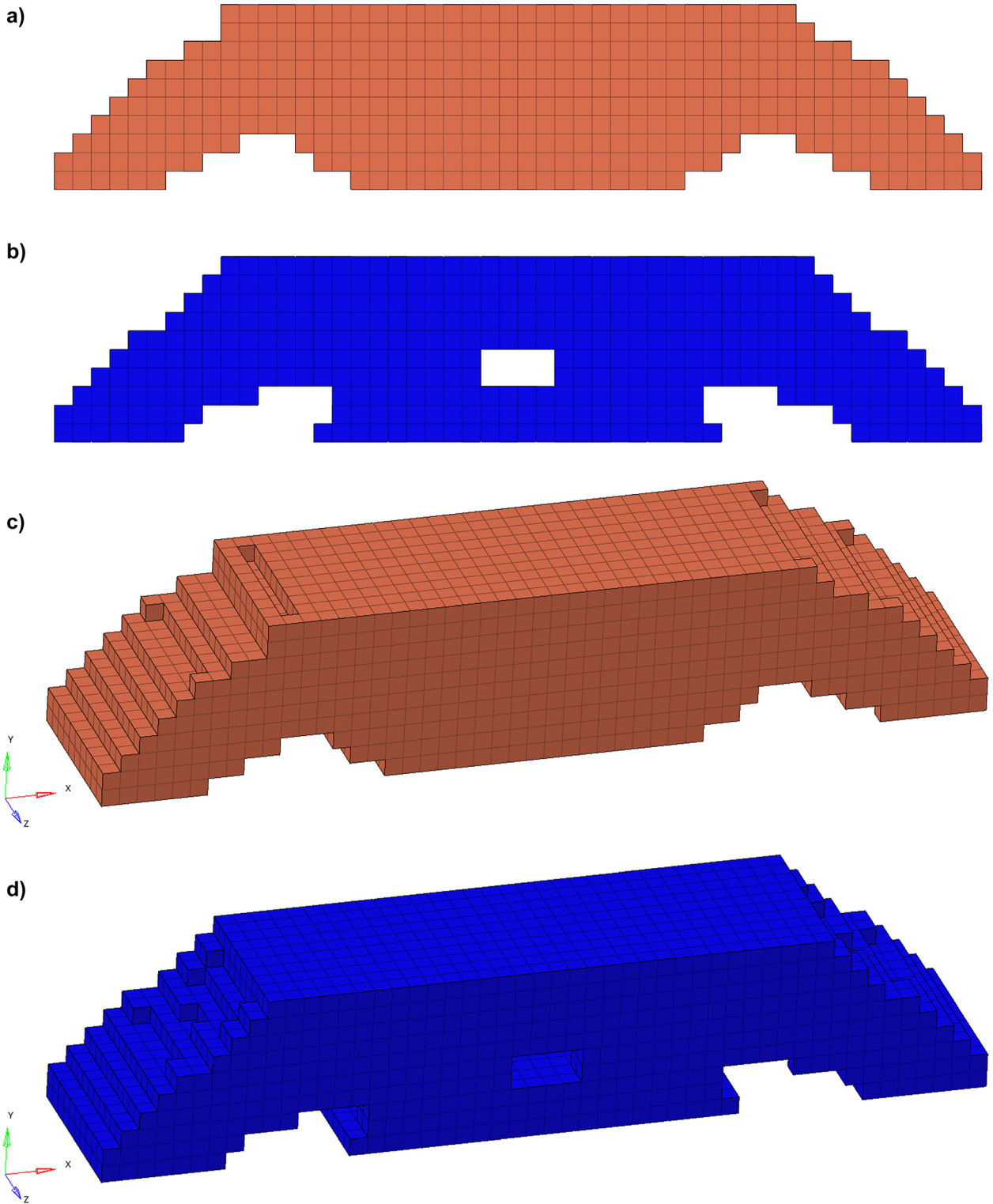


Figure 7: MBB beam, a) front view of the optimum topology obtained with Optistruct, b) front view of the optimum topology obtained with IGEA, c) Isometric view of the optimum topology obtained with Optistruct, d) Isometric view of the optimum topology obtained with IGEA.

Figure 11 depicts the final topologies obtained using IGEA and Optistruct. Figure 11a and b show that the circumference of the region constrained by the boundary

condition is formed in a similar way. Also, Figure 11c and d show that the material distribution around the hole is similar. On the other hand, since the optimization

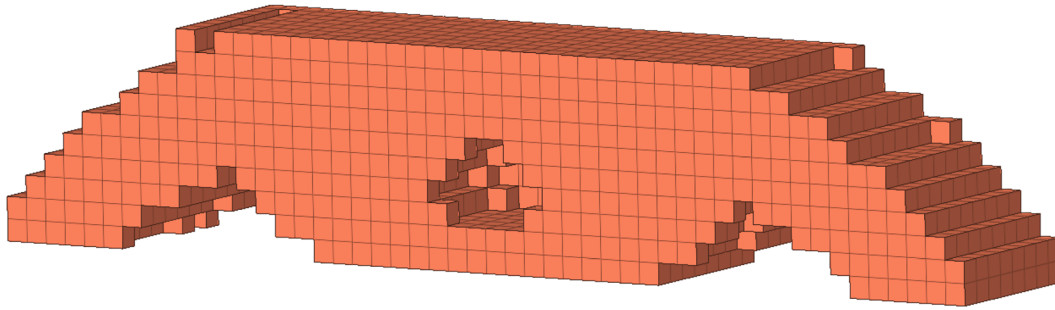


Figure 8: The gap in the middle of the optimum design attained by Optistruct.

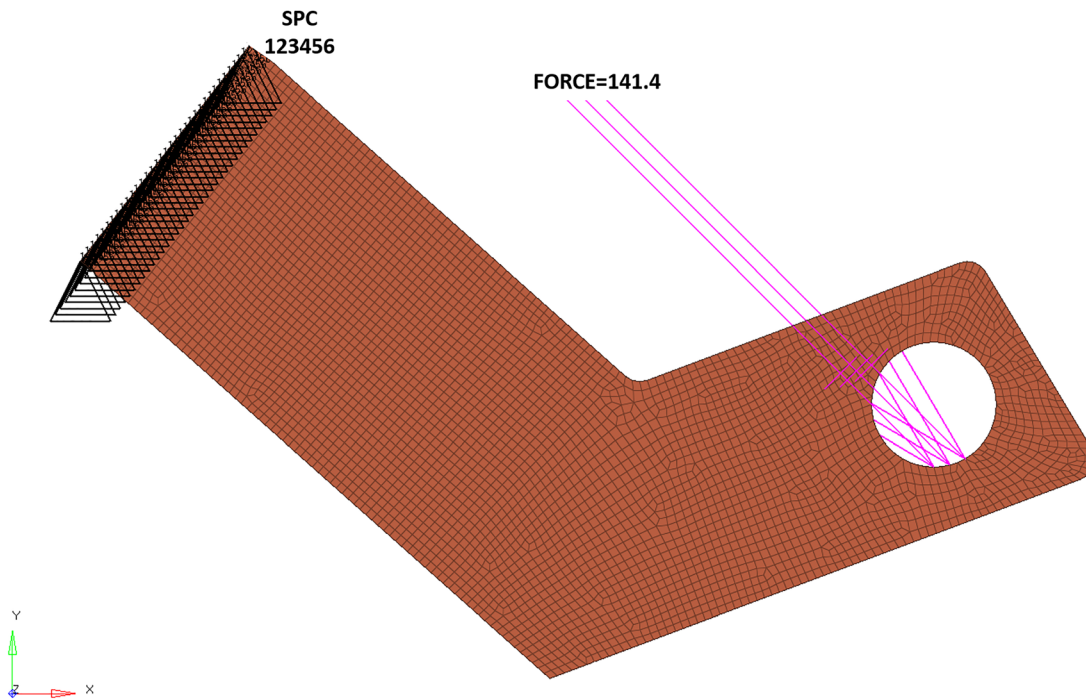


Figure 9: Initial design, loading and boundary conditions for the aviation bracket problem.

Table 1: Mechanical properties of AlSi10Mg powder used in production (SLM Solutions, AlSi10Mg).

	Manufacturing angle	Mean	Standard deviation
Modulus of elasticity (GPa)	0° (horizontal)	58	5
	45°	63	12
	90° (vertical)	52	4
Yield strength (MPa)	0° (horizontal)	152	5
	45°	155	4
	90° (vertical)	150	6

algorithms of IGEA and Optistruct are different, there exist apparent differences in the final topologies.

To provide another comparison, an additional imaging filter (a property available in Optistruct) is

applied to the Optistruct results. Figure 12 depicts a comparison of the IGEA results and “additionally filtered” Optistruct results. The optimization results are now more similar.

It is also noteworthy that the additional display filter is used for post-processing, but can manipulate results incorrectly. For example, when the additionally filtered results in Figure 13 are examined, it is seen that some of the elements with an artificial density value of 0 are still preserved in the design, while some elements of the elements with a higher density value are deleted. Therefore, comparison of the raw results of the Optistruct is more meaningful.

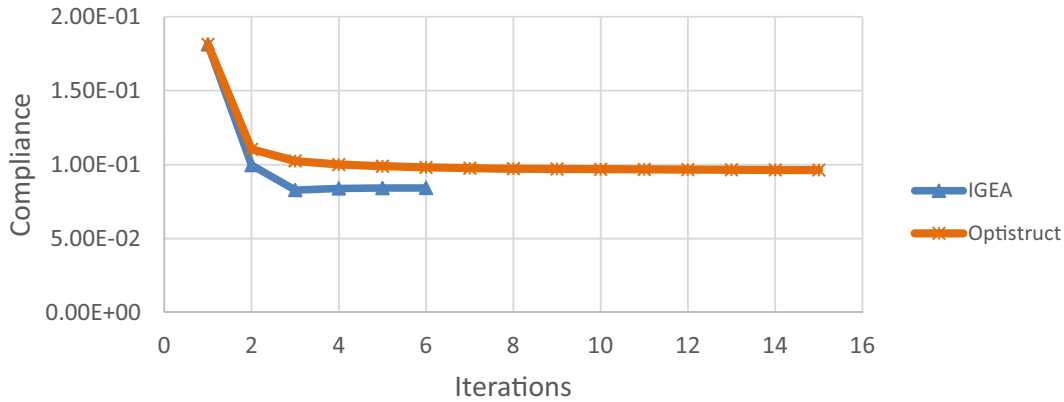


Figure 10: Variation of the objective function with respect to iterations, for the aviation bracket design problem.

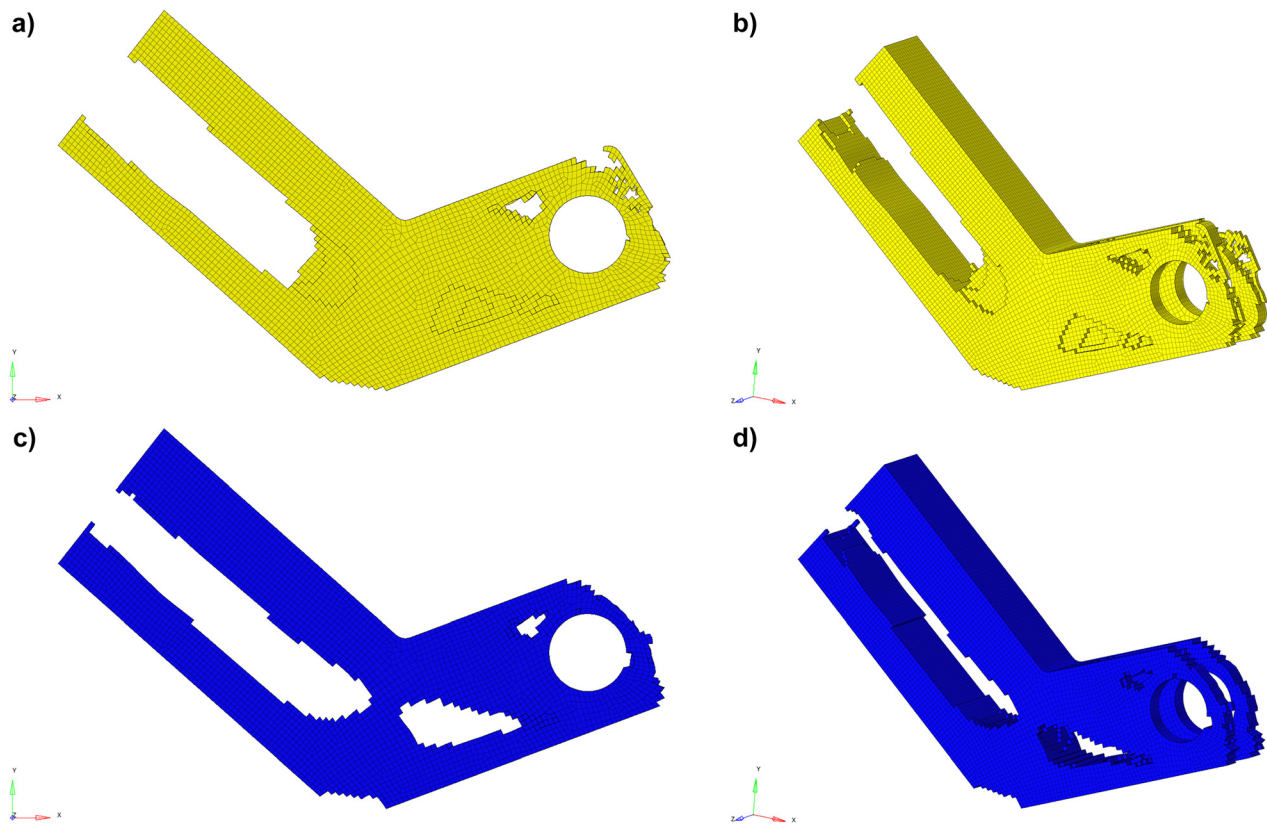


Figure 11: Aviation bracket, a) front view of the optimum topology obtained with Optistruct, b) front view of the optimum topology obtained with IGEA, c) Isometric view of the optimum topology obtained with Optistruct, d) Isometric view of the optimum topology obtained with IGEA.

5 Conclusions

In this study, a topology optimization framework, which has a modular structure and works fully automatically using MATLAB software, was developed. The performance of the proposed framework is tested on two popular academic topology optimization problems, followed by an industrial application problem, and compared to that of

the Optistruct software. From the results obtained, the following conclusions could be drawn:

- For the academic problems, it was observed that IGEA provided smaller lower objective function values than Optistruct, and converges to the optimum result in fewer iterations. In addition, when the optimum topologies were compared, they were very similar. These examples validated the IGEA.

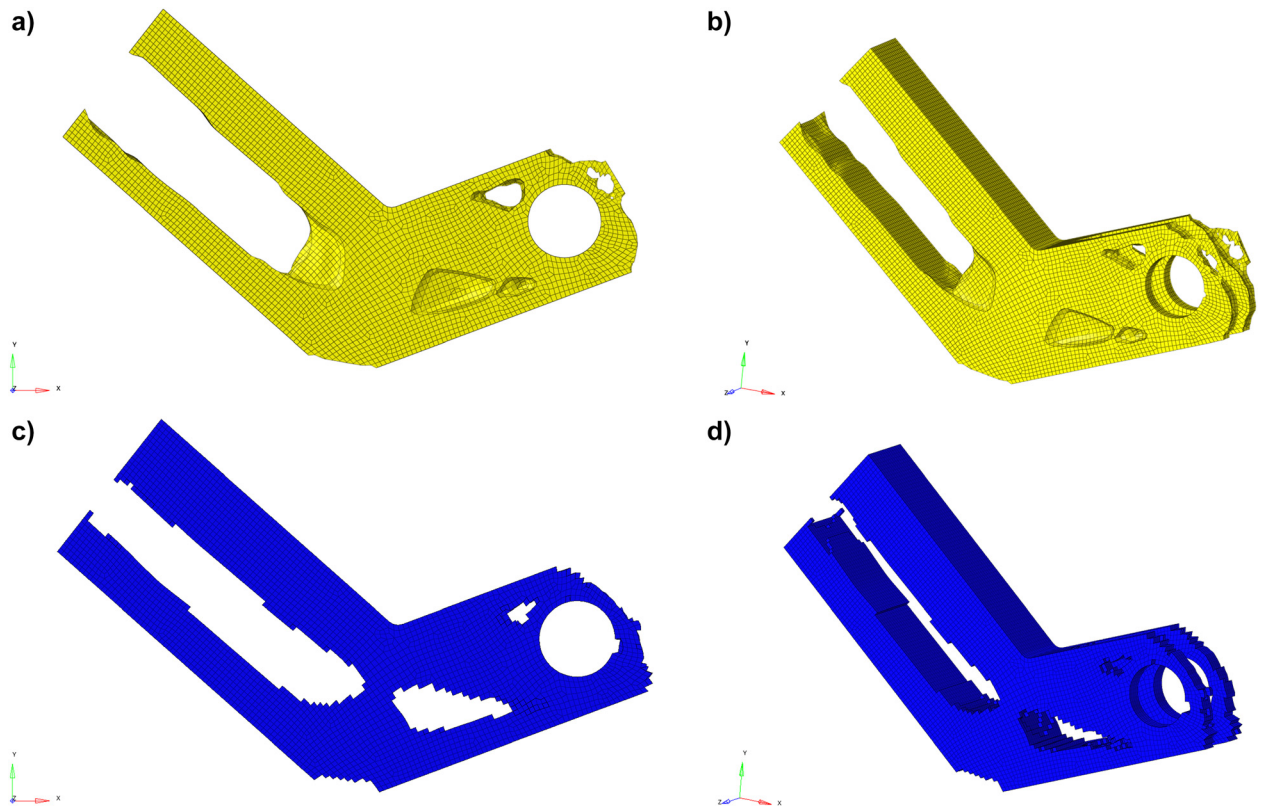


Figure 12: Aviation bracket, a) front view of the optimum topology obtained with Optistruct, b) front view of the optimum topology obtained with IGEA, c) Isometric view of the optimum topology obtained with Optistruct, d) Isometric view of the optimum topology obtained with IGEA.

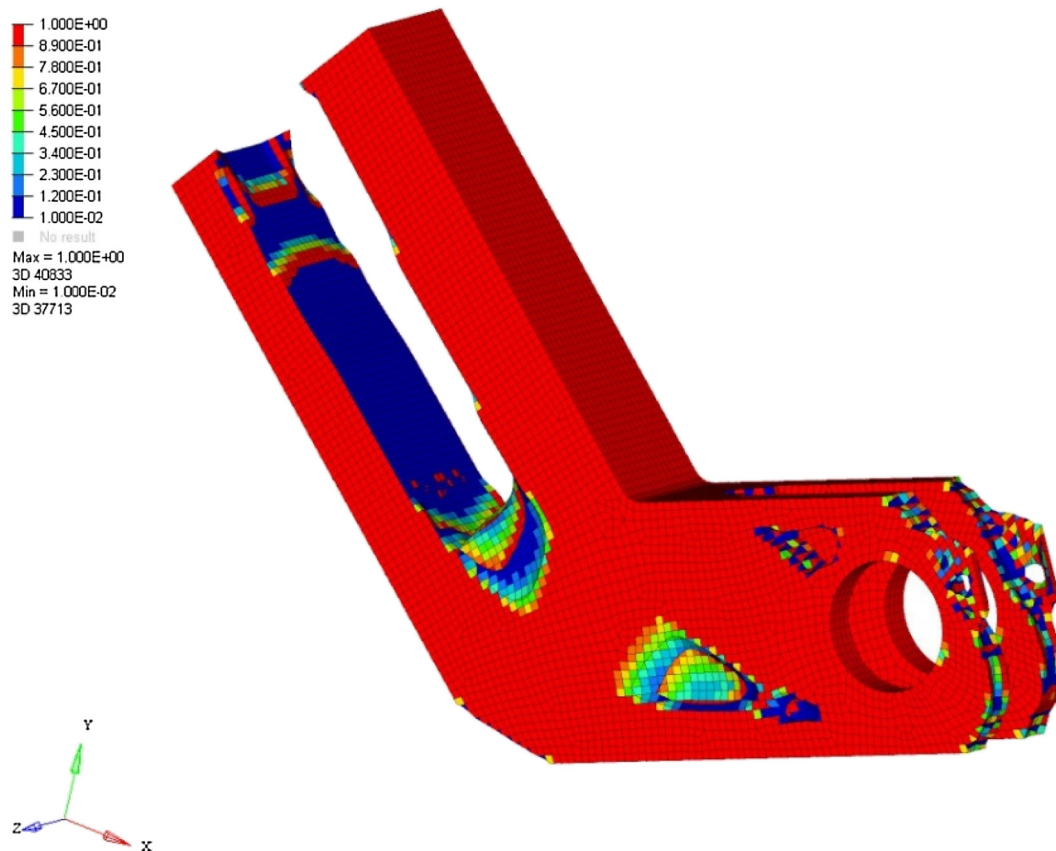


Figure 13: Artificial density distribution of the result with the additional imaging filter for the aviation bracket problem.

- For the aerospace bracket problem, it was found that the optimum compliance value obtained using IGEA was 0.87 times smaller than that of the Optistruct. Also, IGEA converged to the optimum in six iterations, whereas Optistruct converged in 15 iterations.

In additive manufacturing, the position of the part relative to the table has a substantial effect on the mechanical properties. Therefore, it is technologically important to develop a topology optimization framework that can handle uncertainties. IGEA has a modular structure that could support the ability to design under uncertainty, and by further developing IGEA reliability-based and/or robust topology optimization frameworks could be developed.

Author contribution: All the authors have accepted responsibility for the entire content of this submitted manuscript and approved submission.

Research funding: None declared.

Conflict of interest statement: The authors declare no conflicts of interest regarding this article.

References

- [1] R. T. Haftka and Z. Gürdal, *Elements of Structural Optimization*, 3rd ed. Dordrecht, Netherlands, Kluwer Academic Publishers, 2012.
- [2] A. Kaveh, R. Sheikholeslami, S. Talatahari, and M. Keshvari-Ilkhichi, “Chaotic swarming of particles: a new method for size optimization of truss structures,” *Adv. Eng. Software*, vol. 67, pp. 136–147, 2014, <https://doi.org/10.1016/j.advengsoft.2013.09.006>.
- [3] B. Aslan and A. R. Yıldız, “Optimum design of automobile components using lattice structures for additive manufacturing,” *Mater. Test.*, vol. 62, no. 6, pp. 633–639, 2020, <https://doi.org/10.3139/120.111527>.
- [4] R. T. Haftka and R. V. Grandhi, “Structural shape optimization—a survey,” *Comput. Methods Appl. Mech. Eng.*, vol. 57, no. 1, pp. 91–106, 1986, [https://doi.org/10.1016/0045-7825\(86\)90072-1](https://doi.org/10.1016/0045-7825(86)90072-1).
- [5] B. S. Yıldız, A. R. Yıldız, E. İ. Albak, H. Abderazek, S. M. Sait, and S. Bureerat, “Butterfly optimization algorithm for optimum shape design of automobile suspension components,” *Mater. Test.*, vol. 62, no. 4, pp. 365–370, 2020, <https://doi.org/10.3139/120.111492>.
- [6] M. P. Bendsøe and O. Sigmund, *Topology Optimization: Theory, Methods, and Applications*, Berlin, Germany, Springer, 2004.
- [7] M. P. Bendsøe and N. Kikuchi, “Generating optimal topologies in structural design using a homogenization method,” *Comput. Methods Appl. Mech. Eng.*, vol. 71, no. 2, pp. 197–224, 1988, [https://doi.org/10.1016/0045-7825\(88\)90086-2](https://doi.org/10.1016/0045-7825(88)90086-2).
- [8] G. Allaire, E. Bonnetier, G. Francfort, and F. Jouve, “Shape optimization by the homogenization method,” *Numer. Math.*, vol. 76, no. 1, pp. 27–68, 1997, <https://doi.org/10.1007/s002110050253>.
- [9] S. Osher and J. Sethian, “Fronts propagating with curvature dependent speed—algorithms based on Hamilton-Jacobi formulations,” *J. Comput. Phys.*, vol. 79, no. 1, pp. 12–49, 1988, [https://doi.org/10.1016/0021-9991\(88\)90002-2](https://doi.org/10.1016/0021-9991(88)90002-2).
- [10] G. Allaire, F. Jouve, and A. M. Toader, “A level-set method for shape optimization,” *C. R. Math.*, vol. 334, no. 12, pp. 1125–1130, 2002, [https://doi.org/10.1016/S1631-073X\(02\)02412-3](https://doi.org/10.1016/S1631-073X(02)02412-3).
- [11] H. A. Eschenauer, V. V. Kobelev, and A. Schumacher, “Bubble method for topology and shape optimization of structures,” *Struct. Optim.*, vol. 8, pp. 42–51, 1994, <https://doi.org/10.1007/BF01742933>.
- [12] J. Sokolowski and A. Zochowski, “On the topological derivative in shape optimization,” *SIAM J. Control Optim.*, vol. 37, no. 4, pp. 1251–1272, 1999, <https://doi.org/10.1137/S0363012997323230>.
- [13] A. Novotny, R. Feijoo, E. Taroco, and C. Padra, “Topological sensitivity analysis,” *Comput. Methods Appl. Mech. Eng.*, vol. 192, nos. 7–8, pp. 803–829, 2003, [https://doi.org/10.1016/S0045-7825\(02\)00599-6](https://doi.org/10.1016/S0045-7825(02)00599-6).
- [14] M. Wallin, M. Ristinmaa, and H. Askfelt, “Optimal topologies derived from a phase-field method,” *Struct. Multidiscip. Optim.*, vol. 45, no. 2, pp. 171–183, 2012, <https://doi.org/10.1007/s00158-011-0688-x>.
- [15] A. Kawamoto, T. Matsumori, S. Yamasaki, et al., “Topology optimization by a time-dependent diffusion equation,” *Int. J. Numer. Methods Eng.*, vol. 93, no. 8, pp. 795–817, 2013, <https://doi.org/10.1002/nme.4407>.
- [16] C. Mattheck and S. Burkhardt, “A new method of structural shape optimization based on biological growth,” *Int. J. Fatig.*, vol. 12, pp. 185–190, 1990, [https://doi.org/10.1016/0142-1123\(90\)90094-U](https://doi.org/10.1016/0142-1123(90)90094-U).
- [17] Y. M. Xie and G. P. Steven, “A simple evolutionary procedure for structural optimization,” *Comput. Struct.*, vol. 49, pp. 885–896, 1993, [https://doi.org/10.1016/0045-7949\(93\)90035-C](https://doi.org/10.1016/0045-7949(93)90035-C).
- [18] Z. Zuo, T. Xie, and X. Huang, “Evolutionary topology optimization of structures with multiple displacement and frequency constraints,” *Adv. Struct. Eng.*, vol. 15, no. 2, pp. 359–372, 2012, <https://doi.org/10.1260/1369-4332.15.2.359>.
- [19] O. Sigmund and K. Maute, “Topology optimization approaches: a comparative review,” *Struct. Multidiscip. Optim.*, vol. 48, pp. 1031–1055, 2013, <https://doi.org/10.1007/s00158-013-0978-6>.
- [20] J. Zhu, H. Zhou, C. Wang, L. Zhou, S. Yuan, and W. Zhang, “A review of topology optimization for additive manufacturing: status and challenges,” *Chin. J. Aeronaut.*, vol. 34, no. 1, pp. 91–110, 2021, <https://doi.org/10.1016/j.cja.2020.09.020>.
- [21] A. R. Yıldız, “Optimal structural design of vehicle components using topology design and optimization,” *Mater. Test.*, vol. 50, no. 4, pp. 224–228, 2008, <https://doi.org/10.3139/120.100880>.
- [22] M. Cavazzuti, A. Baldini, E. Bertocchi, D. Costi, E. Torricelli, and P. Moruzzi, “High performance automotive chassis design: a topology optimization based approach,” *Struct. Multidiscip. Optim.*, vol. 44, no. 1, pp. 45–56, 2011, <https://doi.org/10.1007/s00158-010-0578-7>.
- [23] E. M. Dede, S. N. Joshi, and F. Zhou, “Topology optimization, additive layer manufacturing, and experimental testing of an air-cooled heat sink,” *J. Mech. Des.*, vol. 137, no. 11, 2015, Art no. 111403, <https://doi.org/10.1115/1.4030989>.

- [24] C. B. Dilgen, S. B. Dilgen, D. R. Fuhrman, O. Sigmund, and B. S. Lazarov, “Topology optimization of turbulent flows,” *Comput. Methods Appl. Mech. Eng.*, vol. 331, pp. 363–393, 2018, <https://doi.org/10.1016/j.cma.2017.11.029>.
- [25] L. Cheng, J. Bai, and A. C. To, “Functionally graded lattice structure topology optimization for the design of additive manufactured components with stress constraints,” *Comput. Methods Appl. Mech. Eng.*, vol. 344, pp. 334–359, 2019, <https://doi.org/10.1016/j.cma.2018.10.010>.
- [26] A. R. Yıldız, U. A. Kılıçarpa, E. Demirci, and M. Doğan, “Topography and topology optimization of diesel engine components for light-weight design in the automotive industry,” *Mater. Test.*, vol. 61, no. 1, pp. 27–34, 2019, <https://doi.org/10.3139/120.111277>.
- [27] H. T. Kollmann, D. W. Abueidda, S. Koric, E. Guleryuz, and N. A. Sobh, “Deep learning for topology optimization of 2D metamaterials,” *Mater. Des.*, vol. 196, pp. 1–14, 2020, Art no. 109098, <https://doi.org/10.1016/j.matdes.2020.109098>.
- [28] O. Sigmund, “A 99 line topology optimization code written in Matlab,” *Struct. Multidiscip. Optim.*, vol. 21, no. 2, pp. 120–127, 2001, <https://doi.org/10.1007/s001580050176>.
- [29] K. Liu and A. Tovar, “An efficient 3D topology optimization code written in Matlab,” *Struct. Multidiscip. Optim.*, vol. 50, pp. 1175–1196, 2014, <https://doi.org/10.1007/s00158-014-1107-x>.
- [30] K. Suzuki and N. Kikuchi, “A homogenization method for shape and topology optimization,” *Comput. Methods Appl. Mech. Eng.*, vol. 93, no. 3, pp. 291–318, 1991, [https://doi.org/10.1016/0045-7825\(91\)90245-2](https://doi.org/10.1016/0045-7825(91)90245-2).
- [31] B. Hassani and E. Hinton, “A review of homogenization and topology optimization. I—Homogenization theory for media with periodic structure,” *Comput. Struct.*, vol. 69, no. 6, pp. 707–717, 1998, [https://doi.org/10.1016/S0045-7949\(98\)00131-X](https://doi.org/10.1016/S0045-7949(98)00131-X).
- [32] M. Zhou and G. I. N. Rozvany, “The COC algorithm, part II: topological, geometrical and generalized shape optimization,” *Comput. Methods Appl. Mech. Eng.*, vol. 89, pp. 309–336, 1991, [https://doi.org/10.1016/0045-7825\(91\)90046-9](https://doi.org/10.1016/0045-7825(91)90046-9).
- [33] G. I. N. Rozvany, M. Zhou, and T. Birker, “Generalized shape optimization without homogenization,” *Struct. Multidiscip. Optim.*, vol. 4, no. 3, pp. 250–252, 1992, <https://doi.org/10.1007/BF01742754>.
- [34] H. Mlejnek, “Some aspects of the genesis of structures,” *Struct. Optim.*, vol. 5, pp. 64–69, 1992, <https://doi.org/10.1007/BF01744697>.
- [35] B. Bourdin, “Filters in topology optimization,” *Int. J. Numer. Methods Eng.*, vol. 50, no. 9, pp. 2143–2158, 2001, <https://doi.org/10.1002/nme.116>.
- [36] O. Sigmund, “Morphology-based black and white filters for topology optimization,” *Struct. Multidiscip. Optim.*, vol. 33, pp. 401–424, 2007, <https://doi.org/10.1007/s00158-006-0087-x>.
- [37] P. T. Boggs and J. W. Tolle, “Sequential quadratic programming,” *Acta Numer.*, vol. 4, pp. 1–51, 1995, <https://doi.org/10.1017/S0962492900002518>.
- [38] K. Svanberg, “The method of moving asymptotes—a new method for structural optimization,” *Int. J. Numer. Methods Eng.*, vol. 24, no. 2, pp. 359–373, 1987, <https://doi.org/10.1002/nme.1620240207>.
- [39] P. W. Christensen and A. Klarbring, *An Introduction to Structural Optimization*, Berlin, Germany, Springer, 2009.
- [40] T. Bruns and D. Tortorelli, “Topology optimization of non-linear structures and compliant mechanisms,” *Comput. Methods Appl. Mech. Eng.*, vol. 190, pp. 3443–3459, 2001, [https://doi.org/10.1016/S0045-7825\(00\)00278-4](https://doi.org/10.1016/S0045-7825(00)00278-4).
- [41] SLM Solutions, Material data sheet, Al-Alloy AlSi10Mg, 2021 [Online]. Available: https://www.slm solutions.com/fileadmin/userupload/MDS_Al-Alloy_AlSi10Mg_0619.pdf.

The authors of this contribution

İstemihan Gökdağ

İstemihan Gökdağ received his BSc and MSc degrees in Mechanical Engineering from TOBB University of Economics and Technology in 2017 and 2021, respectively. He works at the Turkish Aerospace Industries Inc., and his main fields of interests include topology optimization and additive manufacturing of aircraft structural components.

Erdem Acar

Dr. Erdem Acar is a professor in the Department of Mechanical Engineering, TOBB University of Economics and Technology, Ankara, Turkey. His research interests include optimization, design of automobile and aircraft structures, finite element analysis, ballistic simulations, and uncertainty analysis. He is an associate fellow of the American Institute of Aeronautics and Astronautics (AIAA) and he has been serving as a Review Editor for the *Journal of Structural and Multidisciplinary Optimization*, Springer, since 2017.